Catalysis Letters Vol. 107, Nos. 1–2, February 2006 (© 2006)
DOI: 10.1007/s10562-005-9724-z

A novel synthesis route of butyric acid from hydrogenation of maleic anhydride over Pd/TiO_2 catalysts

Jian Xu[a], Kunpeng Sun[a], Li Zhang[b], Yunlai Ren[a], and Xianlun Xu[a,*]

[a]*State Key Laboratory for Oxo Synthesis Slective Oxidation, Lanzhou Institute of Chemical physics, Chinese Academy of Sciences, Lanzhou 730000, China*
[b]*PetroChina Lanzhou Lubricating oil R&D Institute, Lanzhou 730060, China*

Received 6 July 2005; accepted 19 November 2005

A highly efficient Pd/TiO_2 catalyst for the liquid phase hydrogenation of maleic anhydride has been prepared by sol–gel method, and super critical fluid of ethanol drying (SCFE) was applied. The catalyst exhibited excellent activity and high yield to butyric acid. The structural properties of TiO_2 supported Pd catalyst were investigated by BET, TEM, XRD, XPS and TPR techniques with the aim of finding a correlation between the structure parameters and the catalytic activities.

KEY WORDS: maleic anhydride; butyric acid; hydrogenation; Pd/TiO_2; sol–gel.

1. Introduction

Hydrogenation of maleic anhydride is of important industrial significance as all its derivatives *viz*., Butyric acid, γ-butyrolactone, succinic acid, succinic anhydride, 1,4-butanediol are commodity chemicals of considerable industrial importance [1,2]. Hydrogenation of maleic anhydride over different noble metals and Cu based catalysts both in vapor and liquid phases have been reported by many research groups [3–6]. In these catalytic systems, γ-butyrolactone and succinic anhydride are the main products, however, the study of hydrogenation of maleic anhydride in liquid phase to butyric acid, that is butyric acid as the main product, has not been reported.

Butyric acid has many applications in the chemical industry as well as the food and the pharmaceutical industries [7–9]. It is used in the form of pure acid to enhance butter-like notes in food flavours. Esters of the acid are used as the additives for increasing the fruit fragrance and as aromatic compound for the production of perfumes. Butyric acid is currently produced by mainly two processes [10,11]: (i) the oxidation of butanol (ii) the fermentation of starch. Butyric acid can be also prepared by the oxidation of aldehyde, maleic anhydride is considered as a feedstock these days because of its availability and lower price due to the construction of large fluidized-bed plants based on A-lusuisse–Lummus Crest and Britist Petroleum Union Chimique Belge technologies. In this paper, a novel synthesis route of butyric acid by hydrogenation of maleic anhydride in liquid phase is proposed.

Sol–gel is a versatile tool for the preparation of more active and selective catalyst. The sol–gel technique has been applied to the preparation of a variety of catalysts including also metals supported on silica and titania [12–14]. Several papers are dedicated to catalytic hydrogenation over sol–gel catalyst [15,16]. In the present work, a 1% Pd/TiO_2 (w/w) catalyst is prepared by sol–gel method, and super critical fluid of ethanol drying (SCFE) is applied. The as-prepared catalysts exhibited superior activity to hydrogenation of maleic anhydride in liquid phase to butyric acid. To compare, other two catalysts with same palladium content were prepared by impregnation and deposition–precipitation.

2. Experimental

2.1. Catalyst preparation

The catalyst prepared by different methods *viz*., sol–gel, impregnation and deposition–precipitation were designated as SG, Imp, and DP, respectively. The SG catalyst was prepared as follows. At 40 °C, a mixed solution of 12 mL ethanol and 2.8 mL solution of palladium chloride (0.17 mmol) was added dropwise within 1 h into 22 mL ethanol containing 0.062 mol tetrabutoxytitanium (TBOT) and 0.062 mol acetic acid. The solution was stirred vigorously for 1 h; after aged over night, the gel was dried under supercritical fluid of ethanol (SCFE) at 260 °C, 8 MPa. The support used in DP and Imp catalysts was prepared by the hydrolysis of TBOT as described in SG catalyst preparation. The TiO_2 support was impregnated with a solution of $PdCl_2$ (0.17 mmol), after impregnation step, the catalyst was

* To whom correspondence should be addressed.

dried at 120 °C over night. Toward the DP catalyst preparation, an aqueous solution of 0.25 M Na_2CO_3 was added drop-wise to an aqueous mixture of $PdCl_2$ and TiO_2 powder until the PH value reached 10 under vigorous stirring. The resulting supension was aged 3 h under stirring, and then was washed several times with distilled water until no chlorine anion was detected in the resine water with a $AgNO_3$ reagent. The resulting precipitate was filtered, dried at 120 °C. All the catalysts were calcined at 500 °C for 2 h and reduced with pure hydrogen at 500 °C before used.

2.2. Catalytic activity test

The activity test was carried out in a 150 mL stainless autoclave. About 40 mmol maleic anhydride, 0.5 g catalyst and 20 mL ethanol were charged in the clave. The reactor was purged with hydrogen three times to remove the air, then it was pressurized up to 3 MPa and heated to 240 °C, once the pressure reached a steady state, the hydrogenation was initiated immediately by stirring the mixture vigorously. After reaction, the products collected were analyzed by gas chromatograph (Shimadazu, GC-Mini3, Japan), in which 20 mm ×0.32 mm (∅) SE-54 capillary column and the flame ionization detector were used.

2.3. Catalyst characterization

BET surface areas of catalysts calculated from the nitrogen adsorption isotherm at 77 K measured in a micrometrics ASAP2010 apparatus. The surface morphology and the particle size were both determined with a TEM (JSM-5600LV Kevex). Temperature programmed reduction was conducted using a 50 mg catalyst (in a fixed-bed quartz reactor) under 10% H_2 in Ar (10 mL/min) with a ramping rate of 10 °C/min from 20 to 600 °C. X-ray diffraction (XRD) data of catalysts were collected on a Rigaku Dmax-B diffractometer (Cu $K\alpha$ radiation, 50 kV, 60 mA). PHI 550 photoelectron spectrometer equipped with an Mg $K\alpha$ ($hv = 1253.6$ eV) was been used for obtaining XPS data. Binding energies were calculated with respect to C 1s at 285.00 eV.

3. Results and discussion

3.1. Effect of preparation method on the hydrogenation of maleic anhydride

Table 1 shows the effect of preparation method on the hydrogenation of maleic anhydride. For both catalysts, 100% conversion of maleic anhydride was achieved after 2 h. The major products consisted of butyric acid and succinic anhydride under the reaction condition. Other products like γ-butyrolactone, 1,4-butanediol or tetrahydrofuran were not detected. The yield of butyric acid reached to 93.5% over SG catalyst, the yield of butyric acid over three catalysts are found to be in the order: SG > DP > Imp. In addition, the hydrogenation of maleic anhydride was tested on the Cu/Zn/Al catalyst under the same condition compared with Pd/TiO_2 catalyst. The yield of γ-butyrolactone reached 82.7% on Cu based catalyst, butyric acid was not detected in the products. These results indicated that the product distribution was decided by the structure property and composition of catalyst.

3.2. Effect of reaction time on the hydrogenation of maleic anhydride

The yield of butyric acid as functions of time over SG, DP and Imp catalysts are plotted in figure 1. A 100% conversion of maleic anhydride can be obtained in only about 5 min over all three different catalysts, and the yield of butyric acid increased steeply up to about 90% in a reaction time of 50 min. After 120 min, the yield of butyric acid reached to 93.5% over SG catalyst. As showing in Scheme 1, the hydrogenation of maleic anhydride to butyric acid probably follows three step reactions [17]. These results indicated that SG catalyst was a excellent catalyst for hydrogenation of maleic anhydride to butyric acid. The activity test shown above implied that the Pd/TiO_2 catalyst had high activity to the first and third step reactions. That is to say, the SG catalyst has highly selective activation of the carbonyl in maleic anhydride or succinic anhydride molecules.

Table 1
The effect of preparation method on the hydrogenation of maleic anhydride

Preparation method	Conversion(%)	Yield(%)		
		Butyric acid	Succinic anhydride	γ-butyrolactone
Sol–gel(SG)	100	93.5	6.5	–
Deposition–precipitation(DP)	100	86.6	13.4	–
Impregnation(Imp)	100	81.3	18.7	–
Cu based catalyst[a]	100	–	6.1	82.7

[a]Cu based catalyst: Cu/Zn /Mg/Cr = 40:5:5:50, atomic ratio %.
Reaction conditions: MA = 40 mmol, catalyst = SG, 0.5 g, H_2 = 3 MPa, Stirrer = 700 rpm, duration = 2 h.

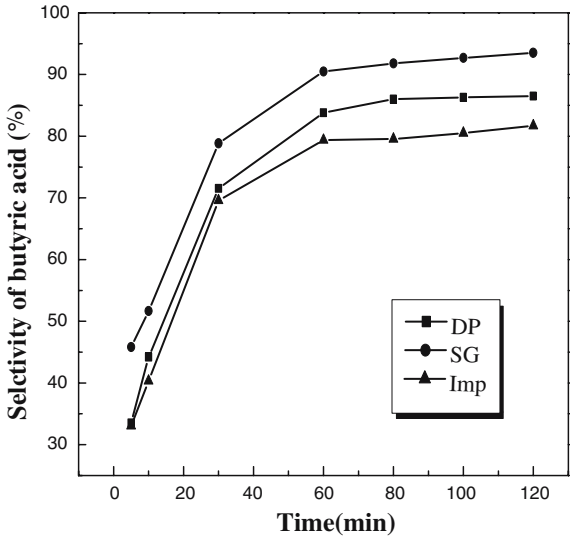

Figure 1. The yield of BA as functions of time over SG, DP and Imp catalysts. Reaction conditions: MA = 40 mmol, catalyst = 0.5 g H_2 = 3 MPa Stirrer = 700 rpm, duration = 2 h.

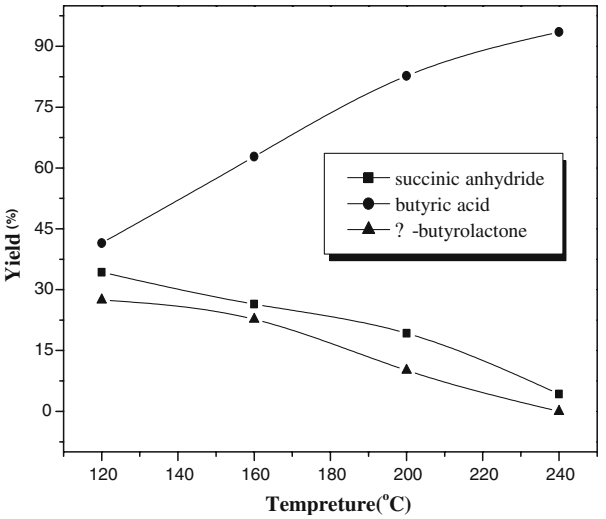

Figure 2. Effect of reaction temperature on the conversion and product distribution in the hydrogenation of maleic anhydride over SG catalyst.

3.3. *Effect of reaction temperature on the product distribution in the hydrogenation of maleic anhydride over SG catalyst*

Figure 2 presents the effect of temperature on the hydrogenation of maleic anhydride over SG catalyst. The yield of butyric acid increased rapidly with a increasing of reaction temperature, when the reaction temperature is below 240 °C, γ-butyrolactone and other side products were detected in the products. These results indicated that increasing reaction temperature was beneficial to the formation of butyric acid.

3.4. *Effect of reduction temperature on the conversion and product distribution in the hydrogenation of maleic anhydride over SG catalyst*

Table 2 shows the effect of reduction temperature on the conversion and product distribution in the hydrogenation of maleic anhydride over SG catalyst. The product distribution over the catalyst reduced at low temperature (573 K) was totally different from that over the catalyst reduced at high temperature (773 K). A large amount of γ-butyrolactone and other products were detected over the catalyst which reduced at low temperature (573 K) under the same reaction condition. This difference might be attributed to the strong metal-support interaction (SMSI) effect that caused by reduction at high temperature for Pd/TiO_2 catalyst. This result indicated that the surface property of Pd had remarkable influence on the yield of butyric acid.

3.5. *Effect of calcinations temperature on the product distribution in the hydrogenation of maleic anhydride over SG catalyst*

The effect of calcination temperature on the product distribution in the hydrogenation of maleic anhydride over SG catalyst were plotted in figure 3. The experimental data about the hydrogenation of maleic anhydride showed a very strong influence of the calcination temperature on the production distribution. When the calcination temperature was below 773 K, butyric acid and succinic anhydride were the main products, and the yield of butyric acid increased with the increasing calcination temperature. However, noticeble changes in the production distribution occurred upon increasing calcination temperature to 773–1073 K, γ-butyrolactone and other products were detected. The yield of butyric acid decreased sharply to 32.8%, and that, the yield of γ-butyrolactone increased to 24.3%.

3.6. *X-ray diffraction (XRD)*

The XRD patterns of calcinated SG, DP and Imp catalysts are shown in figure 4. The major features exhibited on the XRD patterns of the calcinated

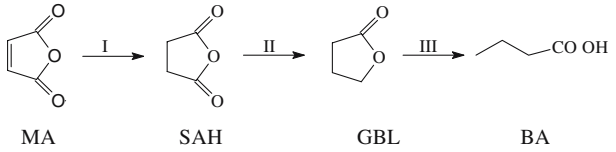

Scheme 1. The path of maleic anhydride hydrogenation to butyric acid.

Table 2
Effect of reducing temperature on maleic anhydride hydrogenation over SG catalyst

Reducing temperature (K)	Conversion (%)	Yield (%)			
		Butyric acid	γ-butyrolactone	Succinic anhydride	Others
573	100	34.4	33.2	7.1	25.3
773	100	93.5	–	6.5	–

Reaction conditions: MA = 40 mmol, catalyst = SG, 0.5 g, H_2 = 3 MPa, Stirrer = 700 rpm, duration = 2 h.

catalysts showed the characters of the anatase form of TiO_2. A weak peak corresponding to PdO at $2\theta \approx 34°$ is observed over SG and DP catalyst, the Pd peak intensity over Imp catalyst is much higher compared to that over SG and DP catalyst, indicating that palladium was more dispersed on SG and DP catalyst. Moreover, the XRD patterns of SG catalysts calcinated at 623, 773, 923, and 1073 K are also shown in figure 5. In the sample treated below 773 K, showed the diffraction line corresponding to anatase form of TiO_2. The rutile form of TiO_2 began to appear from 923 K. When the calcinated temperature was increased to 1073 K, the anatase form of TiO_2 was almost transformed into rutile TiO_2. Based on the XRD results and the experimental data on yield dependence on calcination temperature, we can concluded that the product distribution was markedly influenced by the crystal form of TiO_2. Butyric acid and SAH were the only two products over anatase TiO_2 supported Pd catalyst, and the major product was γ-butyrolactone over rutile TiO_2 supported Pd catalyst.

3.7. Transmission electron microscopy (TEM)

To compare the Pd dispersion of catalysts directly, we have obtained TEM pictures of the reduced catalysts, the TEM morphology of the SG and DP catalysts revealed that the Pd crystallites were homogeneously distributed with the average particle size arroud 6 and 7 nm, respectively as shown in figure 6. It was apparent that Pd particles were highly dispersed on SG and DP catalysts compared with the case of Imp catalyst. The Pd crystallites over Imp catalyst aggregated on support to some extent. This result was in accord with that obtained from XRD.

3.8. Summarized characterization data for Pd/TiO_2 catalyst

Table 3 presents the characteristics of Pd/TiO_2 catalyst. The surface areas of Pd of each catalyst were estimated on the basis of the surface concentration of elements and the BET surface area, assuming that the atomic cross sections are 0.060 nm^2 for Pd, 0.050 nm^2 for O^{2-}, 0.018 nm^2 for Ti, which are calculated from the atomic and ionic radii; that is, the surface area of Pd (S_{Pd}) is calculated by the equation, $S_{Pd} = S_{BET}\alpha_{Pd}c_{Pd}/\alpha_{Pd}c_{Pd} + \alpha_M c_M + c_O$. Here, S_{BET} is BET surface area; α_{Pd} and α_M are atomic ratios of Pd/O and M/O; c_{Pd}, c_M and c_O are the cross section [18]. After impregnation step, the BET surface area of Imp catalyst decreased sharply, and was lower than that of DP and SG catalysts. Moreover, the Pd dispersity of Imp catalyst was lower than that of DP and SG catalysts, these results were in accord with TEM characterization. Based on the activity test and the characteristics of Pd/TiO_2 catalyst shown above, we can concluded that the dispersity and particle size of Pd have no notable influence on the yield of butyric acid.

3.9. X-ray photoelectron spectroscopy (XPS)

XPS spectrum obtained from reduced catalysts are summarized in figure 7. For the SG catalyst, the binding energy of the Pd $3d_{5/2}$ is 335.7 eV which is 0.3 eV higher than that of the metal Pd (335.4 eV) [19,20]. However, that is not true in the case of DP and Imp catalysts, probably, the positive shift in the case of SG catalyst can be attributed to the strong interaction between metal and support [21]. In the case of TiO_2 supported Pd catalyst, the support interacts strongly with Pd after a high temperature reduction (HTR) at 500 °C, the phenomenon is referred to as "the strong metal-support interaction" (SMSI) [22–24]. Moreover, the order of

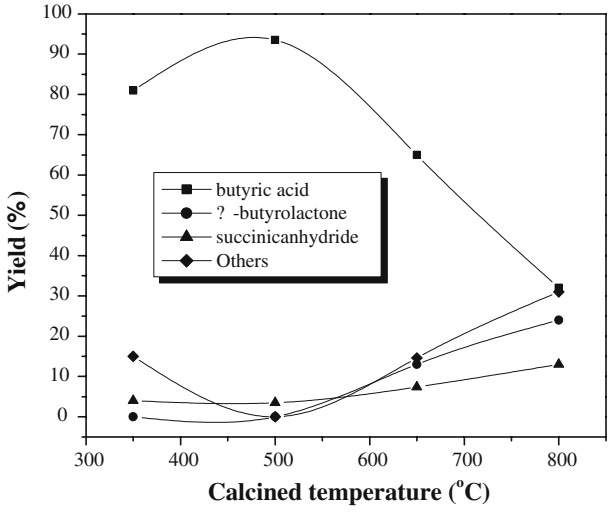

Figure 3. Effect of calcination temperature on the product distribution in the hydrogenation of maleic anhydride over SG catalyst.

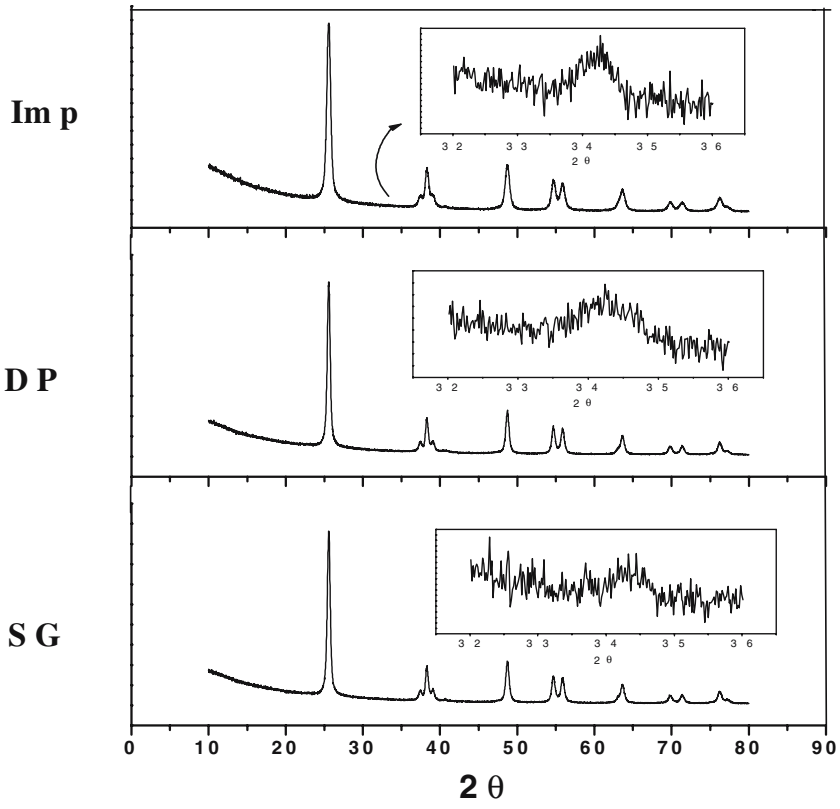

Figure 4. The XRD patterns of three calcinated catalysts.

binding energies values for Pd $3d_{5/2}$ over three catalysts are found to be in accord with that of activity test shown above. This result suggests that the yield of butyric acid extremely depend on the interaction between metal support. Dandekar and Albert Vannice [25] suggested that some organic molecules containing carbonyl bonds, such as acetone, crotonaldehyde, and phenylacetaldehyde can adsorbed more strongly *via* the C=O bond in di-σ mode on inter facial Pd (or Pt)–TiO_x sites created on these catalyst during HTR, the oxygen in the carbonyl groups is envisioned to be coordinated with either Ti^{+3} (or Ti^{+2}) cations at these interfacial sites with the C atom stabilized on a neighboring Pd (or Pt) site, thus leading to a di-σ_{CO} adsorption configuration. The strong adsorption of maleic anhydride or succinic anhydride species *via* the C=O bond in di-σ mode on inter facial Pd–TiO_x site favors the nucleophilic attack of the carbon by hydrogen dissociatively adsorbed on Pd, leading to enhanced hydrogenation activity of the carbonyl group and consequently superior selectivity in maleic anhydride hydrogenation to butyric acid.

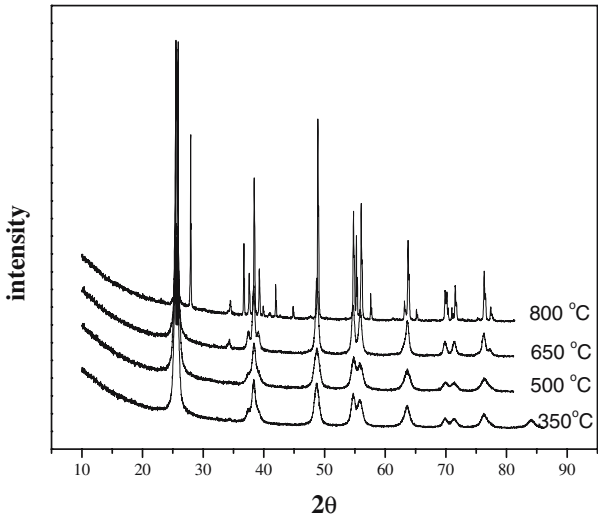

Figure 5. The XRD patterns of SG catalysts calcinated at different temperature.

3.10. Temperature programmed reduction (TPR)

To further understand the origin of highly selective activation of the carbonyl in maleic anhydride or succinic anhydride over Pd/TiO_2 catalyst, H_2-TPR and XPS spectra of three catalysts are obtained. H_2-TPR profiles of the different catalysts and TiO_2 are shown in figure 8. Although the TPR profiles exhibited similar spectra, variations (peak intensity and peak position) existed between samples. Reduction of Pd started about 60 °C and ended below 160 °C. The peak (α) can be attributed to the reduction of Pd^{2+}. The TPR profile of

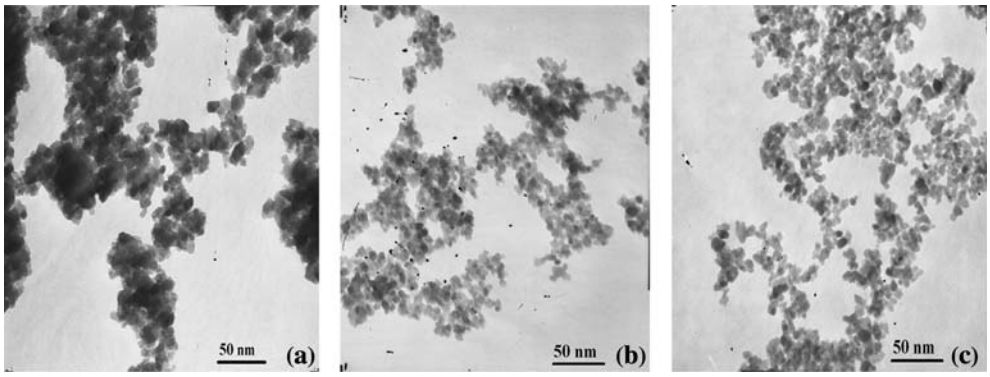

Figure 6. TEM photos of three reduced catalysts (a) TEM photo of Imp sample (b) TEM photo of DP sample (c) TEM photo of SG sample.

Table 3
Characteristics of Pd/TiO_2 catalyst

Catalyst code	BET surface area (m^2/g catalyst)	Pore diameter (Å)	Pd surface area (m^2/g catalyst)	Pd dispersity on surface (%)[a]	Pd particle size (nm)[b]
SG	103.3	81.5	0.68	0.91	7.5
DP	108.5	86.4	1.79	1.65	6.2
Imp	59.8	94.1	0.54	0.65	15.4

[a]Defined by S_{Pd}/S_{BET}.
[b]Evaluated from the FWHM using the Scherrer equation.

blank TiO_2 shows a broaden peak at 400 °C, resemble peaks (γ) appeared at the TPR profiles of three catalysts, this result shows that Ti^{4+} can be reduced to Ti^{3+}. Besides (α and γ) peak, a third peak (β) appeared at about 350 °C at the TPR profiles of three catalysts, this result suggest that Ti^{4+} can be reduced to Ti^{3+} in the presence of Pd even at lower reduction temperature, which is caused by the dissociatively chemsorbed hydrogen on palladium diffusing from Pd to TiO_2 and reducing Ti^{4+} to Ti^{3+} [26–28]. For SG, DP and Imp catalysts, the maxima center of the α peak appeared at

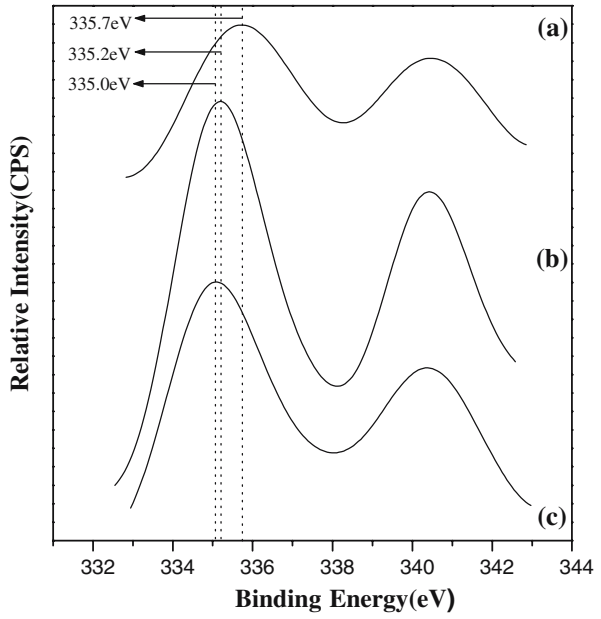

Figure 7. XPS of Pd $3d_{5/2}$ for reduced catalysts. (a) SG (b) DP (c) Imp.

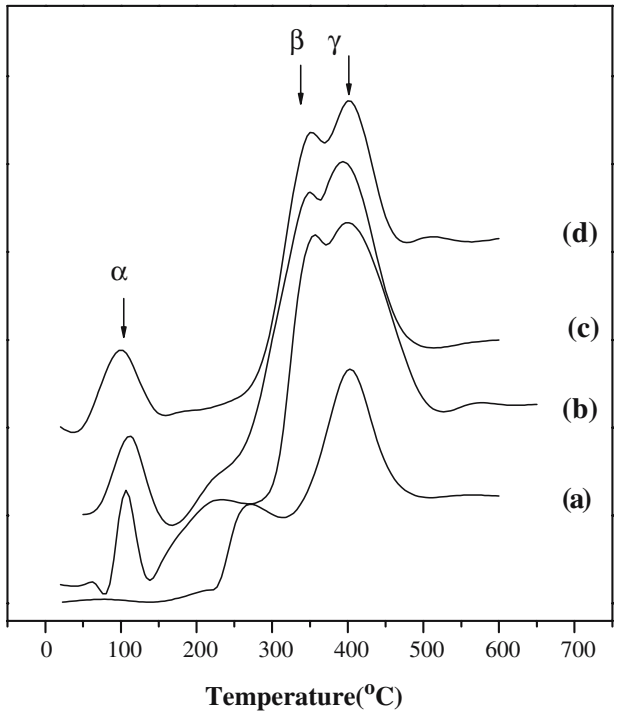

Figure 8. Temperature programmed profiles of Pd/TiO_2 catalysts and blank TiO_2: (a) blank TiO_2 (b) Imp (c) SG (d) DP.

about 111.2, 106.1 and 100.8 °C, respectively, the α peak of SG catalyst was shifted to higher temperature. This result suggested that the interaction of Pd between support was strengthened for three catalysts with different preparation methods. Combining the activity test shown above, we deduced that the yield of butyric acid probably depend on the interaction between metal and support.

4. Conclusion

The Pd/TiO_2 catalyst prepared by sol–gel was proved to be an excellent catalyst for selective hydrogenation of maleic anhydride in liquid phase to butyric acid. At 240 °C, 93.5% yield to butyric acid and 100% conversion of maleic anhydride were obtained over SG catalyst. The dispersity and particle size of Pd had no obvious influence on the yield of butyric acid. The product distribution was mainly determined by the reaction temperature and the crystal forms of TiO_2. The high conversion of maleic anhydride and high yield towards butyric acid were attributed to the strong adsorption of maleic anhydride or succinic anhydride species via the C=O bond in di-σ mode on inter facial Pd–TiO_x site which induced by the high temperature reduced step.

References

[1] N. Harris and M.W. Tuck, Hydrocarb. Process 69 (1990) 79.
[2] R. Lancia, A. Vaccari, C. Fumagalli and E. Armbruster, US Patent 5698713.
[3] U.R. Pillai, E.S. Demessie and D. Yong, Appl. Catal. B. Environ. 43 (2003) 131.
[4] S.M. Jung, E. Godard, S.Y. Jung, K.C. Park and J.U.K. Choi, J. Mol. Catal. 198 (2003) 297.
[5] U.R. Pillai, E.S. Demessie, Chem. Comm. 2002, 422.
[6] G.L. Castiglioni, M. Ferrari, A. Guercio, A. Vaccari, R. Lancia and C. Fumagalli, Catal. Today 27 (1996) 181.
[7] D. Vandak, J. Zigova and E.S. Schlossers, Process Biochem. 32 (1977) 245.
[8] Y. Zhu, Z.T. Wu and S.T. Yang, Process Biochem. 38 (2002) 657.
[9] S.E. Lower, Seifen Oele Fette Wachse 117 (1991) 403.
[10] J. Zigova, E. Sturdik and D. Vandak, Process Biochem. 34 (1999) 835.
[11] Y.L. Chen and T.C. Chou, J. Appl. Electrochem. 26 (1996) 543.
[12] R.D. Gonzalez, T. Lopez and R. Gomez, Catal. Today 35 (1997) 293.
[13] W. Zou and R.D. Gonzalez, Catal. Lett. 12 (1992) 73.
[14] H.D. Gesser and D.C. Goswami, Chem. Rev. 89 (1985) 765.
[15] P. Reyes, G. Pecchi and J.L.G. Fierro, Langmuir 17 (2001) 522.
[16] J. Hájek, N. Kumar, T. Salmi and D.Y.U. Murzin, Ind. Eng. Chem. Res. 42 (2003) 295.
[17] S.M. Jung, E. Godard, S.Y. Jung, K.C. Park and J.U.K. Choi, Catal. Today 87 (2003) 171.
[18] Y. Usami, K. Kagawa, M. Kawazoe, H. Sakurai and M. Haruta, Appl. Catal. A 171 (1998) 123.
[19] T. Pillo, R.Z. Mann, P. Steiner and S. Hufner, J. Phys. Condens. Matter. 9 (1997) 3987.
[20] M. Burn, A. Berthet and J.C. Bertolini, J. Electron. Spectron. Relat. Phenom. 104 (1999) 55.
[21] R.P. Fernández, J. Concha, I. Pecchi, G. Lopez Granados and M. Fierro, Appl. Catal. A Normal 136 (1996) 231.
[22] S.J. Tauster, S.C. Fung and R.L. Garten, J. Am. Chem. Soc. 100 (1978) 170.
[23] J.K.A. Clarke, R.J. Dempsey, T. Baird and J.J. Rooney, J. Catal. 126 (1990) 370.
[24] S.J. Tauster and S.C. Fung, J. Catal. 55 (1978) 29.
[25] A. Dandekar and M. Albert Vannice, J. Catal. 183 (1999) 344.
[26] J.C. Conesa and J. Soria, J. Phys. Chem. 86 (1982) 1392.
[27] T. Haizinga and R. Prins, J. Phys. Chem. 85 (1981) 2156.
[28] Y. Li, Y. Fan, H.P. Yang, B.L. Xu and M.F. Yang, Chem. Phys. Lett. 372 (2003) 160.